

Chemical Vapor Deposition Growth of 5 mm Hexagonal Single-Crystal Graphene from Ethanol

*Xiao Chen*¹, *Pei Zhao*², *Rong Xiang*¹, *Sungjin Kim*¹, *JinHyeok Cha*¹, *Shohei Chiashi*¹,
Shigeo Maruyama^{1,3*}

¹ Department of Mechanical Engineering,
The University of Tokyo, 7-3-1 Hongo, Bunkyo-ku, Tokyo, 113-8656, Japan

² Institute of Applied Mechanics,
Zhejiang University, 38 Zheda Rd, Hangzhou, 310027, China

³ Energy NanoEngineering Laboratory,
National Institute of Advanced Industrial Science and Technology (AIST), 1-2-1 Namiki,
Tsukuba, 205-8564, Japan

*Corresponding author. E-mail: maruyama@photon.t.u-tokyo.ac.jp (Shigeo Maruyama),
TEL: +81-3-5841-6421, Fax: +81-3-5800-6983

Abstract

We show that graphene single crystals as large as 5 mm can be synthesized from ethanol via chemical vapor deposition (CVD). Key conditions for the successful reduction in nucleation density are extremely low partial pressure of ethanol vapor and pre-oxidation of Cu substrates. The resulting graphene flakes are predominantly homogeneous single-layer hexagons, as characterized by Raman spectroscopy and selected area electron diffraction. However, the edge of ethanol produced graphene shows an armchair feature, suggesting a possible different mechanism from conventional methane CVD.

1. Introduction

Chemical vapor deposition (CVD) synthesis of graphene on poly-crystalline Cu foils has been intensively investigated in the past few years [1-5]. Graphene films synthesized in this way were often poly-crystalline, with typical graphene single-crystal domain sizes of about tens of microns. The numerous grain boundaries in these films decrease both the electrical and mechanical quality of graphene films [6, 7]. Driven by the superior properties of structurally perfect graphene films, major efforts have been aimed at enlarging the sizes of single-crystal graphene domains to millimeter and even centimeter scale [8-14]. To achieve this, many researchers focused on reducing the partial pressure of the carbon source, tuning the C:H ratio, smoothing the Cu surface, as well as adjusting oxygen content of Cu substrates [12-14]. In most of these methods, methane was used as the carbon source and high ratio of H₂ flow is often needed in order to reach equilibrium between growth and etching. Searching for an alternative to methane may be beneficial to both the fundamental understanding of the growth process and the future industrial scale production. In this paper, we report that ethanol can also be utilized to synthesize single crystal graphene up to 5 mm, with very low concentration of H₂. We show that very low partial pressure of ethanol and pre-oxidation of Cu foils are critical to the successful synthesis of the large crystal graphene. At the same time, the edge of ethanol produced graphene shows an armchair feature, suggesting a possible different growth mechanism from conventional methane CVD.

2. Experimental methods

Single layer graphene was grown using alcohol catalytic chemical vapor deposition

(ACCVD) [5]. Here we apply a homemade thermal CVD system, using a quartz tube as the reaction chamber. Briefly, commercial copper foils (Nilaco Corp., CU-113303) were cleaned using IPA, acetone, and HCl, and heated in air on a hot plate at about 250 °C to oxidize the Cu surface. Afterwards, the foil was folded into a Cu pocket, loaded into the CVD chamber, and placed at the center of the furnace. Then the system was vacuumed to approximately 25 Pa by a mechanical pump for 10 minutes. Afterwards, the CVD chamber was heated to the reaction temperature (1065 °C) with an Ar flow under the pressure of 300 Pa. After reaching 1065 °C, the Ar flow was replaced by a 300 sccm flow of 3% H₂ diluted in Ar (partial pressure of H₂ is 10 Pa), and a 0.03 sccm ethanol vapor flow was also introduced into the system to initiate the growth. The total pressure is kept 300 Pa. Depending on the size of graphene flakes desired, the required CVD time could be 2-24 hours.

3. Results and discussion

3.1 Growth of large single-crystal graphene from ethanol

Figure 1a shows an optical image of graphene hexagons on a Cu foil. This sample was heated in air to create a contrast between graphene-covered Cu and bare Cu [13]. A typical scanning electron microscopy (SEM) image of a graphene flake is shown in Figure 1b. In general, these graphene flakes are of hexagonal shapes, with edge-to-edge sizes about several mm. A core of multi-layer graphene at the center of each large graphene flake can be often observed, occupying 10% of the total area of each graphene domain. Assuming each graphene flake grows from one single nucleus, the nucleation density in these samples is roughly 0.2 mm⁻². After transferring the graphene flakes to Si/SiO₂ substrates (Figure 1c), Raman scattering was measured on randomly selected

locations (Figure 1d). The spectra are all characteristic of single-layer graphene (SLG), with a large 2D/G ratio and negligible D-peak. Note that previous reports showed that the Raman spectrum of twisted bi-layer graphene (BLG) could also have a strong 2D-band [15], so the 2D/G ratio is not definitive evidence for the existence of SLG. However, there is a very strong contrast between SLG and BLG on Si/SiO₂ substrates when observed with an optical microscope, and recent studies have shown that a small blue-shift can be observed in the Raman feature of BLG compared with that of SLG [15, 16]. Since there is often a multi-layer core at the center of each flake, we examined the BLG areas with Raman scattering (inset in Figure 1d), and did observe a small blue-shift (5 to 20 cm⁻¹), which is consistent with previous research. Combining the evidences of Raman spectra and optical micrographs, we can unambiguously conclude that the graphene flakes reported in this work are predominantly single-layer.

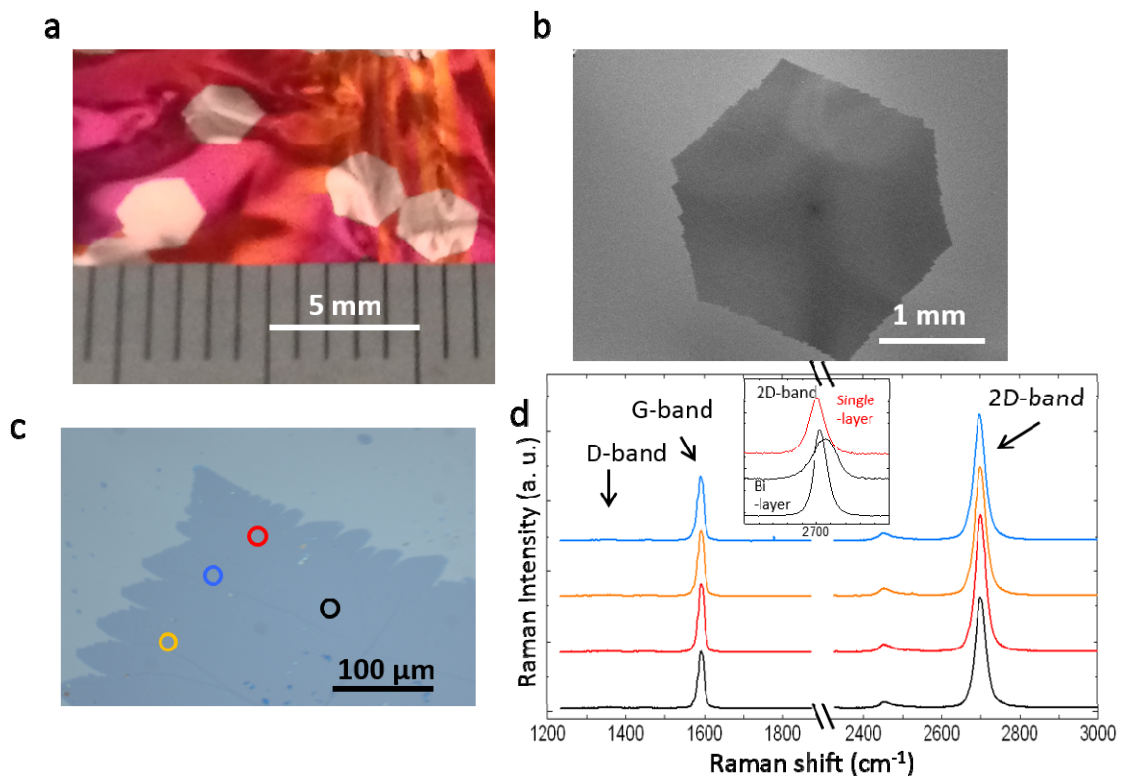


Figure 1. Characterization of hexagonal graphene. a) Optical image of graphene on Cu foil after CVD and oxidation in air. b) Typical SEM image. c) Optical microscopy image of the graphene flake after transfer to Si/SiO₂ substrate. Note that the edge shape is smoother for smaller flakes. d) Raman spectra corresponding to four randomly chosen locations shown in c). Inset in d) is a comparison of the 2D-band of single-layer graphene and bi-layer graphene. The growth conditions are:

To demonstrate the single-crystal nature of these graphene flakes over millimeter scale, we transferred these to transmission electron microscope grids, and performed selected area electron diffraction (SAED). Figure 2b to 2h show the SAED patterns on 8 random locations as shown in Figure 2a, and the maximum rotation in these 8 pattern is smaller than 1.4°, suggesting the single-crystal nature of this graphene flake with a size over 3 mm. The small rotation angle may originate from twisting or folding in the transfer process.

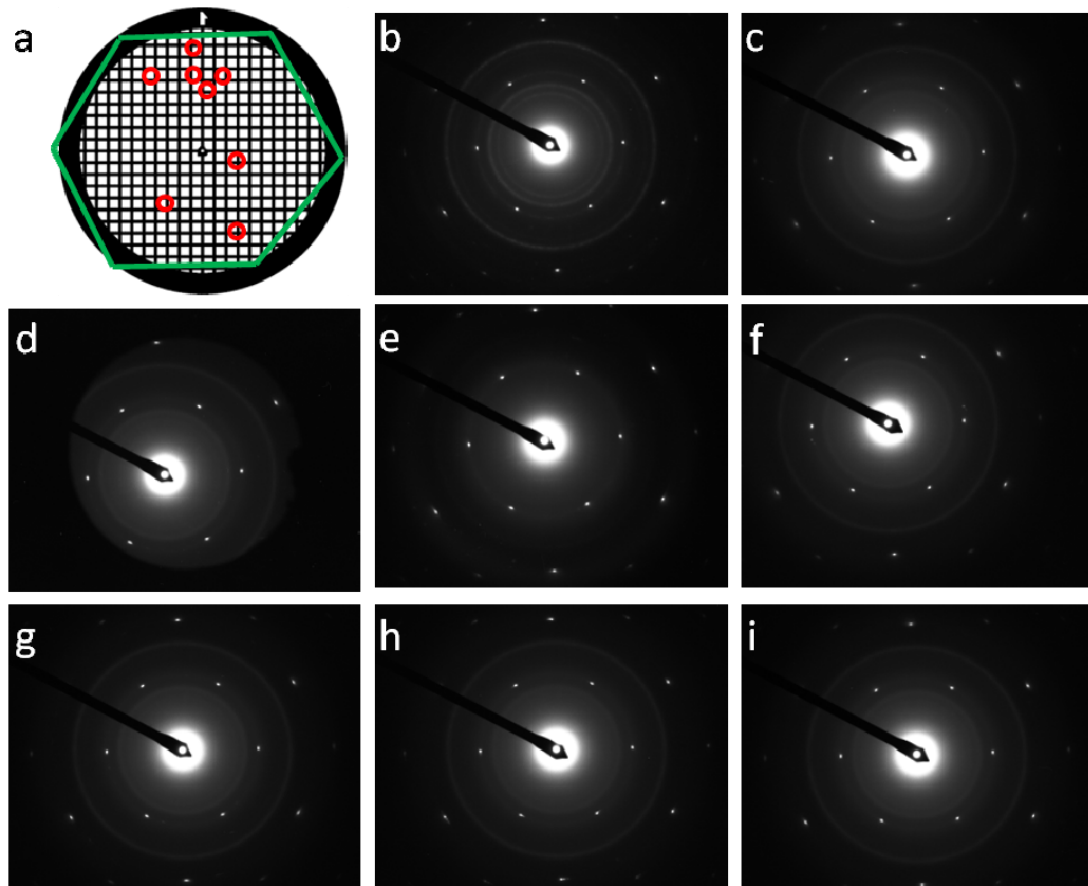


Figure 2. SAED characterization of as-grown graphene. a) The approximate positions of the transferred graphene flake and the locations where SAED patterns are measured. b) to i) SAED patterns on the 8 locations as marked in a). The sample characterized here is grown using the same condition as in Figure 1.

3.2 Oxygen etching and armchair edge

A closer look at these graphene hexagons (Figure 1c) reveals that the edges are much rougher than those grown using atmospheric pressure CVD (APCVD) or CVD using a high concentration of H_2 with methane as the precursor [9-14]. Many dendritic branches can be observed, especially at each corner of the hexagon where the angle is much sharper than 120° . This dendritic shape indicates that the growth is diffusion limited,

rather than reaction limited as was the case in most previous works [9, 11-13]. Scanning Raman spectroscopy was employed to measure a graphene flake transferred to a Si/SiO₂ substrate in order to demonstrate the quality of the graphene flakes (Figure 3). The D-band map is very uniform, with intensity close to the background. A few exceptions were regions of small holes and wrinkles that could be caused by the transfer procedure. Note that unlike most reported results, the intensity of the D peak at the edges of our graphene flakes is very high, especially at the growth fronts (point C in Figure 3f), which is almost the same as the intensity of the G peak. At the valley parts on the edges (point B in Figure 3f), the D-band intensity is much weaker. The D peak originates from a double resonance process [17]. When an electron is created by a photon, it is inelastically scattered by a large momentum phonon to an inequivalent Dirac valley. Then the electron is return to the original valley with an elastic backscattering process, and by rejoining its companion hole while emitting a Raman light, a Raman round trip is completed [18]. The backscattering can only proceed perpendicular to the edge of graphene. So for zigzag edges, elastic backscattering cannot allow the electron return to its original valley in the momentum space, so the Raman emission cannot occur. But an armchair edge can have the backscattering in the right direction. Hence, zigzag edges contribute very little to D-band intensity, and armchair edges raise very high D peak, and this theory has been verified by multiple literatures both theoretically and experimentally [19-21]. So the strong D peak at the edges of our graphene can be best explained as that the graphene edges at these growth fronts are armchair edges. On the other hand, almost all previous works report zigzag graphene edges [8, 9, 11-14], with no obvious rise of D-band intensity and showing a G/D ratio > 10 at the edges. We believe this difference can be explained by a double-etchant mechanism.

Conventionally, a high concentration of H₂ is needed during CVD growth of graphene hexagons in order to balance the growth and etching rates at these growth fronts. This helps maintain the general hexagonal shape even as the flake grows to millimeter sizes. For low pressure CVD with methane/H₂, the partial pressure of H₂ varies from 20 Pa to hundreds of Pa [8-14, 22], and most groups apply pure H₂ in these procedures. In the case reported here, we use a low partial pressure of dilute H₂ (3%, 10 Pa). On the other hand, there is an oxygen atom in each ethanol molecule, which can also serve as an etchant in the growth of graphene, helping to maintain the oxygen balance in CVD reactions, as has been indicated in the ACCVD growth of single-walled carbon nanotubes. It is possible that at the growth fronts, the armchair structure is more stable for the oxygen etchant, and at the valley parts (point B in Figure 3f), a zigzag edge is more stable for the hydrogen etchant. This theory is very consistent with the recent findings by S. Choubak et al., in which they conclude that in low pressure CVD growth of graphene, oxygen species are the main etchant [23]. The exact mechanism of this procedure is still unclear, and shall be investigated with experiments in the future.

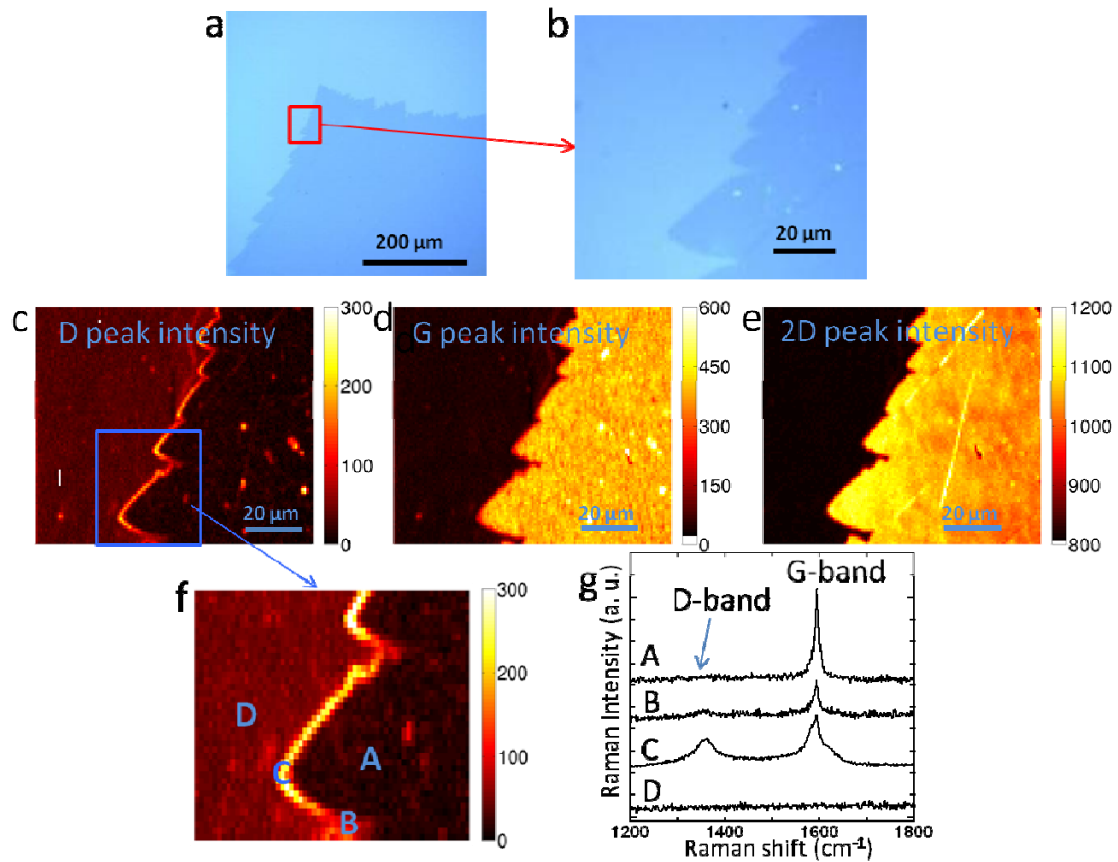


Figure 3. Scanning Raman characterization. a) and b), optical microscope image of graphene transferred on Si/SiO₂ substrate. c), d) and e), Raman maps of the D-, G- and 2D- peak intensity of the same area in b). f), the Raman map of D-peak intensity with higher resolution of the area marked in c). g), Raman spectra of four points marked in c). The sample characterized here is grown using the same condition as in Figure 1.

3.3 Effect of pre-oxidation

There are two essential technical issues in the growth procedure for the low nucleation density of graphene: the ultra-low partial pressure (flow rate) of ethanol vapor, and the thermal oxidation of Cu foils prior to the CVD process. Figures 4a and

4b show the density of graphene nuclei as a function of the partial pressure of ethanol. When applying the ethanol partial pressure of 10 Pa, as reported in a previous work by our group [5], we observe a nucleation density of about 150 mm⁻². When the pressure of ethanol is decreased to 0.03 Pa, the nucleation density is reduced to approximately 8 mm⁻², more than one order of magnitude lower. Furthermore, the shape of each graphene flake is very hexagonal compared with those shown in Figure 4a. The hexagonal shape may originate from the orientation of the graphene lattice, which means that the graphene domains obtained under this condition might be single-crystal. This nucleation-density evolution dependence on the partial pressure of carbon sources is consistent with many previous works [8-12].

On the other hand, the role of surface oxygen is not yet clear. Since 2013, many groups realized that involving oxygen in the CVD reaction can efficiently reduce the nucleation density, and several procedures were developed to add oxygen into the system [14, 22]. Here, we use the method of heating the copper foil on a hot plate in an ambient environment at 250 °C prior to the CVD procedure (pre-oxidation). The copper surface changes from shiny red to dull gray, suggesting the formation of a thin oxide layer on the surface. A clear dependence on the pre-oxidation duration can be observed, as shown in Figure 4. Without any pre-oxidation, we observe a nucleation density of ~8 mm⁻² (Figure 4c), corresponding to an average grain size of ~300 μm. Pre-oxidation for 15 minutes would reduce the nucleation density to ~0.8 mm⁻² (Figure 4d), and further oxidation, for instance at 250 °C for 30 minutes, results in a density of ~0.3 mm⁻² (Figure 4e). With optimized conditions (pre-oxidation for 90 minutes), graphene domains as large as 5 mm are obtained (Figure 4f), with a nucleation density of ~0.1 mm⁻². A higher oxidation temperature with a shorter duration (300 °C, 40 min), or a

lower temperature with a longer duration (240 °C, 2 hours) can result in the similar nucleation density. But if the oxidation is stronger than the optimized one, for instance 250 °C for 2 hours, during the CVD reaction, the Cu pocket would melt along with part of the quartz tube that is adjacent to it, which is very dangerous and unsuitable for the growth. We are not sure the reason behind this melting, but due to this, a nucleation density of $\sim 0.1 \text{ mm}^{-2}$ is the lowest we can get based on this recipe. Though at this stage it is difficult to quantify the exact amount of oxygen in the Cu foil or the thickness of the oxide layer before reaction, this simple pre-oxidation strategy is surprisingly effective to tune the nucleation density and yield mm-scale graphene single crystals.

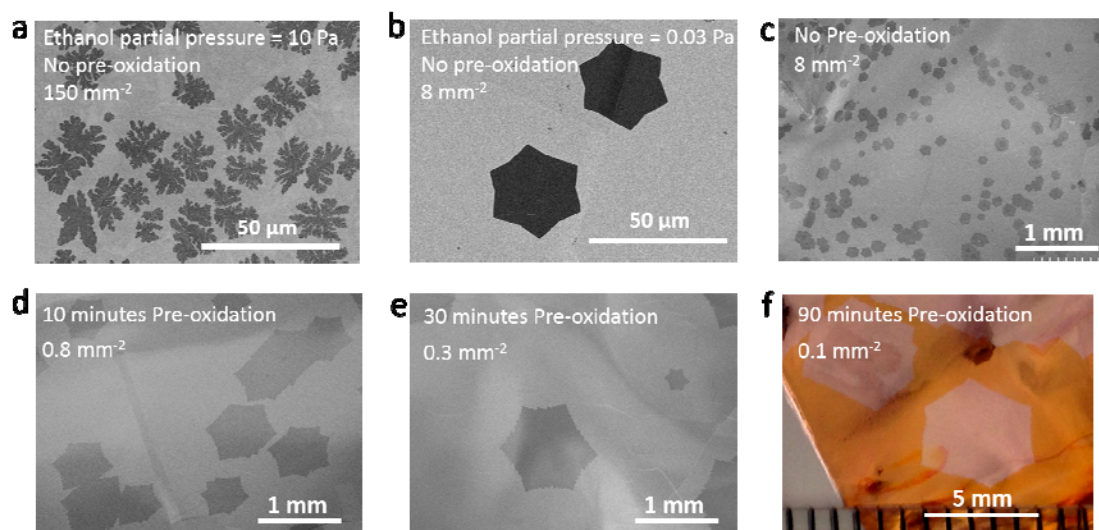


Figure 4. Dependence of nucleation density on ethanol partial pressure and pre-oxidation duration. a) and b) show the effect of ethanol partial pressure with no pre-oxidation procedure. c), d), e) and f) show the effect of different pre-oxidation durations when applying the same ethanol partial pressure of 0.03 Pa. The growth durations are: a) 30 seconds, b) 20 min, c) 40 min, d) 6 hours, e) 8 hours, and f) 22 hours.

Although it is believed that oxygen plays a critical role in decreasing the nucleation density of graphene, the exact mechanism, (e.g. position, chemical stages, concentration of oxygen), of its function is not yet fully clear. For example, G. Eres and colleagues claimed that after a pre-oxidation, a following H₂ reduction removes impurities and heal the defects on Cu surface [22]. However in our process, we directly start the ethanol vapor along with the diluted H₂, without involving any annealing process under high concentration of H₂, and we still achieved very low nucleation density.

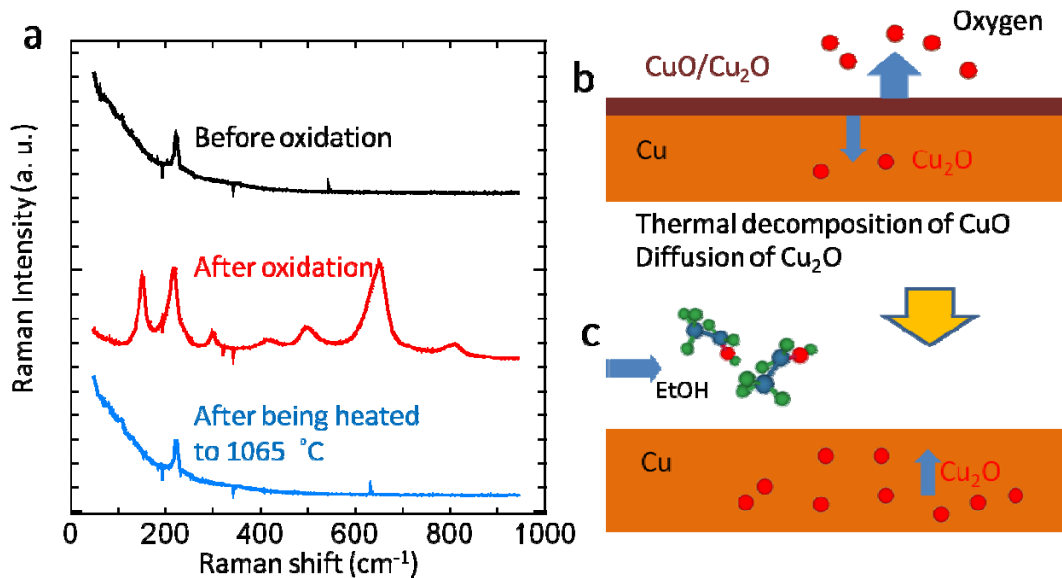


Figure 5. a) Raman spectroscopy of Cu surfaces before oxidation, after oxidation, and after being heated to 1065 °C. b) and c), possible mechanism of the oxide layer on Cu surfaces.

We employed Raman scattering to study the change of the oxide layer on Cu surfaces (Figure 5a). Without any oxidation, a peak near 220 cm⁻¹ can be observed, corresponding to the strong Raman spectral feature of Cu₂O [24], which suggests originally there is a natural oxidation on pristine Cu. After being oxidized, multiple strong peaks in the Raman spectrum were observed, which represents the existence of

both CuO and Cu₂O [24, 25]. After heating to 1065 °C in Ar and immediately cooling down, these strong peaks of CuO and Cu₂O disappear, and only the peak at 220 cm⁻¹ remains, which is almost the same as pristine Cu. Considering that the decomposition temperature of CuO is very low [26], almost all the CuO would be decomposed into other oxides such as Cu₂O during the heating process. On the other hand, Cu₂O is very stable, even in a high-temperature environment, but Raman spectroscopy indicates that the concentration of oxide on Cu surfaces after heating is very low, close to that on pristine Cu. Possibly, during heating, the oxide layer diffuses into the bulk Cu, resulting in an oxygen-rich Cu foil in general as shown in Figure 5b. However, we are not sure of the exact form of oxide at this stage, which could be nano particles or clusters, as often observed in as-purchased commercial copper film [27]. At the later stage when carbon source is supplied, the diffused oxide can be involved in the reaction on the Cu surface. This would result in passivation of potential nucleation sites on the Cu surface [14], which leads to a decrease in the nucleation density.

Besides the decrease in the nucleation density, one other effect of oxygen is believed to be accelerating the growth of graphene flakes by enhancing the detachment of H atoms from the graphene edges [14, 28] and increasing the dissociative adsorption probability of CH₄ [29, 30]. However, in our case, we don't observe an obvious increase in the growth rate with stronger oxidation of the Cu foils. There are two possible reasons for this: first, as discussed in 3.2, the edges of graphene is terminated with oxygen rather than hydrogen; second, there is a constant supply of oxygen from the carbon source, so the effect of pre-added oxygen in Cu foils on the later growth stage is not so obvious.

Since there is an oxygen atom in each ethanol molecule, and ethanol also fully

decomposes at the CVD temperature, the decomposed oxygen-containing species (mainly water) in the chamber may also play an important role in balancing the surface oxygen concentration, as has been discussed in the synthesis of single-walled carbon nanotubes [31, 32]. Literature also showed that a small amount of residue oxygen can decouple graphene from Cu through intercalation during the CVD reaction [33], so the oxygen from ethanol can result in a very weak interaction between Cu and graphene, which may help to explain why the oxygen-terminated armchair edges are more stable in such atmosphere. However, it is difficult to quantify the oxygen from ethanol and those from pre-oxidation, and to distinguish their effects. Just as in the synthesis of single-walled carbon nanotubes, the multiple roles of ethanol need further investigation.

4 Conclusions

Graphene single crystals as large as 5 mm were synthesized using the ACCVD method. Key parameters were: ethanol partial pressure as low as 0.03 Pa, and a 90-minute pre-oxidation procedure in air. The low defect, homogeneous, and single-crystal nature of the resultant graphene flakes has been characterized by scanning Raman spectroscopy and SAED. This proposed CVD procedure only requires a low concentration (3%) of H₂, corresponding to a partial pressure of merely 3 Pa.

Acknowledgment

We thank Professor Erik Einarsson (SUNY Buffalo) for helpful discussion. A part of this work was financially supported by Grants-in-Aid for Scientific Research (22226006, 25107002, 15H02219) and IRENA Project by JST-EC DG RTD, Strategic International

Collaborative Research Program, SICORP. We also acknowledge supports from Center for Nano Lithography & Analysis (The University of Tokyo) supported by 'Nanotechnology Platform' (project No. 12024046) of MEXT, Japan. A part of this work was also supported by 'Global Center for Excellence for Mechanical Systems Innovation' (The University of Tokyo); and VLSI Design and Education Center (VDEC), The University of Tokyo, in collaboration with Cadence Corporation.

References

1. Li X, Cai W, An J, Kim S, Nah J, Yang D, et al. Large-Area Synthesis of High-Quality and Uniform Graphene Films on Copper Foils. *Science* 2009; 324 (5932): 1312-1314.
2. Bhaviripudi S, Jia X, Dresselhaus MS; Kong J Role of Kinetic Factors in Chemical Vapor Deposition Synthesis of Uniform Large Area Graphene Using Copper Catalyst. *Nano Letters* 2010; 10 (10): 4128-4133.
3. Bae S, Kim H, Lee Y, Xu X, Park J-S, Zheng Y, et al. Roll-to-roll production of 30-inch graphene films for transparent electrodes. *Nat Nano* 2010; 5 (8): 574-578.
4. Vlasiouk I, Regmi M, Fulvio P, Dai S, Datskos P, Eres G, et al. Role of Hydrogen in Chemical Vapor Deposition Growth of Large Single-Crystal Graphene. *ACS Nano* 2011; 5 (7): 6069-6076.
5. Zhao P, Kumamoto A, Kim S, Chen X, Hou B, Chiashi S, et al. Self-Limiting Chemical Vapor Deposition Growth of Monolayer Graphene from Ethanol. *The Journal of Physical Chemistry C* 2013; 117 (20): 10755-10763.
6. Yu Q, Jauregui LA, Wu W, Colby R, Tian J, Su Z, et al. Control and characterization of individual grains and grain boundaries in graphene grown by chemical vapour deposition. *Nat Mater* 2011; 10 (6): 443-449.
7. Huang PY, Ruiz-Vargas CS, van der Zande AM, Whitney WS, Levendorf MP, Kevek JW, et al. Grains and grain boundaries in single-layer graphene atomic patchwork quilts. *Nature* 2011; 469 (7330): 389-392.
8. Li X, Magnuson CW, Venugopal A, Tromp RM, Hannon JB, Vogel EM, et al. Large-Area Graphene Single Crystals Grown by Low-Pressure Chemical Vapor Deposition of Methane on Copper. *Journal of the American Chemical Society* 2011; 133 (9): 2816-2819.
9. Yan Z, Lin J, Peng Z, Sun Z, Zhu Y, Li L, et al. Toward the Synthesis of Wafer-Scale Single-Crystal Graphene on Copper Foils. *ACS Nano* 2012; 6 (10): 9110-9117.
10. Chen S, Ji H, Chou H, Li Q, Li H, Suk JW, et al. Millimeter-Size Single-Crystal Graphene by

- Suppressing Evaporative Loss of Cu During Low Pressure Chemical Vapor Deposition. *Advanced Materials* 2013; 25 (14): 2062-2065.
11. Mohsin A, Liu L, Liu P, Deng W, Ivanov IN, Li G, et al. Synthesis of Millimeter-Size Hexagon-Shaped Graphene Single Crystals on Resolidified Copper. *ACS Nano* 2013; 7 (10): 8924-8931.
 12. Zhou H, Yu WJ, Liu L, Cheng R, Chen Y, Huang X, et al. Chemical vapour deposition growth of large single crystals of monolayer and bilayer graphene. *Nat Commun* 2013; 4, 2096.
 13. Gan L, Luo Z, Turning off Hydrogen To Realize Seeded Growth of Subcentimeter Single-Crystal Graphene Grains on Copper. *ACS Nano* 2013; 7 (10): 9480-9488.
 14. Hao Y, Bharathi MS, Wang L, Liu Y, Chen H, Nie S, et al. The Role of Surface Oxygen in the Growth of Large Single-Crystal Graphene on Copper. *Science* 2013; 342 (6159): 720-723.
 15. Zhao P, Hou B, Chen X, Kim S, Chiashi S, Einarsson E, Maruyama S, Investigation of Non-Segregation Graphene Growth on Ni via Isotope-Labeled Alcohol Catalytic Chemical Vapor Deposition. *Nanoscale*, 2013; 5: 6530-6537.
 16. Jorio A, Cançado LG, Raman spectroscopy of twisted bilayer graphene. *Solid State Communications* 2013; 175-176: 3–12.
 17. Thomsen C, Reich. S. Double resonant Raman scattering in graphite, *Phys. Rev. Lett.* 2000; 85: 5214-5217
 18. Basko DM, *Phys. Rev. B: Condens. Matter Mater. Phys.* 2009; 79: 205428-205452
 19. Cancado LG, Pimenta MA, Neves BRA, Dantas MSS, Jorio A, *Phys. Rev. Lett.* 2004; 93: 247401-247405
 20. Malarda LM, Pimenta MA, Dresselhaus G, Dresselhaus MS, *Raman Spectroscopy in Graphene. Physics Reports* 2009; 473: 51–87.
 21. Krauss B, Nemes-Incze P, Skakalova V, Biro LP, Klitzing K, von Smet JH, *Raman Scattering at Pure Graphene Zigzag Edges. Nano Lett.* 2010; 10: 4544–4548.
 22. Eres G, Regmi M, Rouleau CM, Chen J, Ivanov IN, Puzos AA, et al. Cooperative Island Growth of Large-Area Single-Crystal Graphene on Copper Using Chemical Vapor Deposition. *ACS Nano* 2014; 8 (6): 5657-5669.
 23. Choubak S, Levesque PLP, Gaufres E, Biron M, Desjardins P, Martel R, *Graphene CVD: Interplay Between Growth and Etching on Morphology and Stacking by Hydrogen and Oxidizing Impurities. J. Phys. Chem. C* 2014; 118, 21532-21540.
 24. Solache-Carranco H, Juarez-Diaz G, Galvan-Arellano M, Martinez-Juarez J, Romero-Paredes G; Pena-Sierra R, *Raman scattering and photoluminescence studies on Cu₂O, Electrical Engineering, Computing Science and Automatic Control, 2008. CCE 2008, 2008; pp. 421-424.*
 25. Chrzanowski J, Irwin JC, *Raman scattering from cupric oxide. Solid State Communications* 1989; 70 (1): 11-14.

26. Goswami A; Trehan YN The Thermal Decomposition of Cupric Oxide in vacuo. Proceedings of the Physical Society. Section B 1957; 70 (10): 1005.
27. Davis JR, Copper and copper alloys. ASM International, 2001.
28. Terasawa T, Saiki K; Effect of vapor-phase oxygen on chemical vapor deposition growth of graphene. Appl. Phys. Express 2015; 8: 035101.
29. Xing B, Pang X, Wang G; C–H bond activation of methane on clean and oxygen pre-covered metals: A systematic theoretical study. J. Catal. 2011; 282: 74-82.
30. Alstrup I, Chorkendorff I, Ullmann S; The interaction of CH₄ at high temperatures with clean and oxygen precovered Cu(100). Surf. Sci. 1992, 264: 95-102.
31. Maruyama S, Kojima R, Miyauchi Y, Chiashi S; Kohno M Low-temperature synthesis of high-purity single-walled carbon nanotubes from alcohol. Chemical Physics Letters 2002; 360 (3–4): 229-234.
32. Murakami Y, Chiashi S, Miyauchi Y, Hu M, Ogura M, Okubo T, et al. Growth of vertically aligned single-walled carbon nanotube films on quartz substrates and their optical anisotropy. Chemical Physics Letters 2004; 385 (3–4): 298-303.
33. Kidambi PR, Bayer BC, Blume R, Wang ZJ, Baetz C, Weatherup RS, et al.; Observing graphene grow: catalyst-graphene interactions during scalable graphene growth on polycrystalline copper. Nano Lett., 2013, 13 (10): 4769-4778.